Published by
NIGERIAN SOCIETY OF PHYSICAL SCIENCES
Available online @ https://journal.nsps.org.ng/index.php/jnsps

J. Nig. Soc. Phys. Sci. 5 (2023) 1438

Check for updates

Journal of the Nigerian Society of Physical Sciences

Photocatalytic and antibacterial activities of green-mediated *Khaya senegalensis*-silver nanoparticles and oxidized carbon nanotubes

A. H. Labulo[a], A. D. Terna[b,*], O. F. Oladayo[a], H. Ibrahim[a], N. S. Tanko[a], R. A. Ashonibare[c], J. D. Opeyemi[a], Z. Tywabi-Ngeva[d]

[a]*Department of Chemistry, Federal University of Lafia, Lafia, Nasarawa State, Nigeria*
[b]*Department of Chemistry, Federal University of Technology, PMB 1526, Owerri, Imo State, Nigeria*
[c]*Durable Crops Research Department, Nigerian Stored Products Research Institute, P.M.B. 1489, Ilorin, Kwara State, Nigeria*
[d] *Department of Chemistry, Faculty of Science, Centre for Rubber Science and Technology, Nelson Mandela University, Gqeberha, South Africa, 6001.*

Abstract

This study investigated the photocatalytic and antibacterial activities of plant-mediated silver nanoparticles (AgNPs) from a medicinal plant extract of *Khaya senegalensis (K. senegalensis)* and oxygen functionalized carbon nanotubes (oCNTs), respectively. The CNTs were functionalized using acid treatment. The green synthesized AgNPs from *K. senegalensis* (KS-AgNPs) and oCNTs were characterized by UV–Visible spectroscopy, Fourier transform infrared spectroscopy (FTIR), transmission emission microscopy (TEM), scanning electron microscopy (SEM), and X-ray diffraction (XRD). The formation of KS-AgNPs was confirmed by the UV–Vis absorption spectra, which showed an absorption band at 427 nm with a color change from yellow to brown. The morphology of KS-AgNPs was spherical in shape, with an average particle size of 9.30 nm. The FTIR analyses revealed distinctive functional groups, such as, hydroxyl (O-H), amines (N-H), and carbonyl (C-O), which were directly involved in the synthesis and stability of AgNPs. The XRD spectra was distinctive with five intense peaks at 2θ angles of 38.12°, 44.28°, 64.43°, 77.48°, and 81.54° while oCNTs gave intense peaks at 2θ angles of 26.43°, 42.36°, 44.46°, 54.51°, 59.98°, and 77.40°. The photocatalytic property of green synthesized KS-AgNPs was determined to be 40.7 % higher than that of oCNTs when applied for treatment of industrial waste water. The ability of green-mediated KS-AgNPs to inhibit against gram-positive and gram-negative bacteria was observed to be that gram (-) bacteria (*E. coli*) was more susceptible to KS-AgNPs than the gram (+) bacteria (*S. aureus*), in which case their susceptibility was least in oCNTs for both bacteria, respectively.

DOI:10.46481/jnsps.2023.1438

Keywords: *Khaya senegalensis,* silver nanoparticles, carbon nanotubes, photocatalytic, antibacterial activity

Article History :
Received: 08 March 2023
Received in revised form: 01 May 2023
Accepted for publication: 05 May 2023
Published: 22 June 2023

Communicated by: E. A. Emile

1. Introduction

New research suggest to possibilities to create antibacterial and photocatalytic compounds that are more effective and less toxic for usage in order to tackle water pollution, which

*Corresponding author tel. no: +2348100049983
Email address: ternaaugustine2020@gmail.com (A. D. Terna)

is the primary cause of infectious diseases [1]. Producing eco-friendly nanoparticles follows the principles of *green chemistry*, in which naturally existing bioactive chemicals in plants serve as reducing and capping agents while also preserving the environment [2]. By adjusting the concentration of plant extract, it is possible to create shape- and size-dependent nanoparticles under regulated conditions [1], [3]. The treatment of industrial wastewater, in particular that is produced by the textile dying process, is a serious environmental concern. The destruction of organic dyes and bacteria by nanoparticles' catalytic activity makes them potentially useful for the treatment of industrial wastewater [4]. Clean, pure drinking water is currently a major issue due to the rise of so many startup companies and the need to address environmental degradation [5]. Applications for nanoparticles (NPs) in the oxidative degradation of harmful pigments and environmental pollutants seem to be numerous [6]. The enhanced photocatalytic and degrading effectiveness is due to the small, crystalline, particle size, surface clustering, significant optical absorption in the visible range, quick charge transfer, reduced electron-hole charge recombination, and high oxidizing ability of the nanoparticles [7]. NPs have been found to have very sporadic antibacterial action against *S. aureus* and high antibacterial activity against *E. coli* [1]. The combination of surface area, electrostatic interactions between the anionic dye and cationic surface of the nanocatalyst, and the oxidation of polyphenolic/phenolic chemicals or flavonoids present on the surface of the nanoparticles enhances the photocatalytic degradation process of nanoparticles [8]. Moreover, smaller-sized silver nanoparticles (AgNPs) have greater surface areas and more active sites available for the degradation of organic dyes via electron transfer [4]. Further studies have revealed that the high surface-to-mass ratios and unique activities of silver nanoflowers—which are brought on by the high densities of edges, corners, and stepped atoms on their nano-petals—have enhanced photocatalytic qualities over semi-spherical AgNPs [9].

AgNPs made from aqueous leaf extracts have been reported for water remediation [10], as it facilitates the catalytic breakdown of dyes in the presence of visible light [5]. At the moment, bacterial resistance to antimicrobial drugs is the biggest obstacle to treating infectious diseases [10]. AgNPs may infiltrate bacterial cells and injure them by interacting with DNA and other molecules containing phosphorus and sulfur, as silver reacts strongly with these elements. This possibility has been highlighted [10]. The antibacterial effects of AgNPs on bacteria may be caused by their capacity to bind to the surface of bacterial cell membranes and impair the permeability and respiration of the bacterium cell [10]. In wastewater, Gram positive and negative microorganisms are frequently present [4]. It has been demonstrated that gram-negative bacteria are more susceptible to the antibacterial effects of green-mediated AgNPs than gram-positive pathogens [8]. Controlled oxidation is typically used to insert oxygen-containing groups, such as ketone, phenol, lactone, carboxyl group, ether, acid anhydride, etc., to the surfaces of CNTs [11]. The photocatalytic activity of the composite photocatalyst is highly associated with the amount of integrated MWCNTs [12]. MWCNTs have attracted a lot of interest because of their exceptional physical characteristics and adaptable morphologies [13]. As a new class of nanovectors for therapeutic administration, functionalized multi-walled carbon nanotubes (fMWCNTs or oMWCNTs) are demonstrating their effectiveness in the transport and cellular translocation of therapeutic compounds [14], [15], [16]. These f-CNTs can distribute drugs to cells or organs and can be made using one or more bioactive ingredients from the class of compounds that includes peptides, proteins, nucleic acids, and pharmaceuticals [17], [18], [19]. According to the number of concentric layers, CNTs are divided into single-wall (with a typical diameter of 0.4 – 2 nm) and multi-wall (with more layers) (with a typical diameter of 10 – 100 nm) [14]. The carbon nanotube's surface is covered in functional groups, which inhibit undesirable absorption and desorption processes [20], [21], [22], [23]. In this instance, undesirable absorption takes the form of biological medium molecule attachment and potential carbon nanotube content distribution [21]. Since good aqueous stability is a crucial quality for bio-medical applications, CNTs may be more cost-effective and effective than conventional antibiotic therapy because their surfaces can be modified to reduce hydrophobicity and improve adhesion through chemical attachment of proteins and polymers [14]. Gram-positive and gram-negative bacteria are both susceptible to CNTs' antibacterial action [24]. The physical manner of bactericidal action and the generation of oxidative stress, which result in cell membrane damage brought on by the CNTs, are responsible for this activity [24], [25]. The effects of CNTs on infections caused by multidrug-resistant bacteria have been the subject of several in-vitro research [16], [19], [26].

This study was the first to investigate *K. senegalensis* for the production of silver nanoparticles. In order to compare the effectiveness of the photocatalytic and antibacterial activities of green-synthesized silver nanoparticles (KS-AgNPs) and functionalized carbon nanotubes (oCNTs), respectively, a comparative analysis of both materials' properties was conducted when applied for treatment of industrial waste water.

2. Materials and Methods

2.1. Collection of plant materials and waste-water samples

Khaya senegalensis (African mahogany) leaves were collected from Lafia, Nigeria, in February, 2022. Test bacterial species (*Escherichia coli* and *Staphylococcus aureus*) and industrial waste water were procured and sourced from Genetics and Biotechnology Department, Akwa Ibom State University and Eastern Obolo oil producing community, Akwa Ibom, Nigeria, respectively. Silver nitrate ($AgNO_3$) (99.80 %) was purchased from Merck South Africa. Multi-walled-carbon nanotubes (outside diameter 8 – 15 nm, length 15 μm) were obtained from Times Nano. Ltd. (Chengdu, China). All the reagents and chemicals used in this study were of analytical grade. Aqueous solutions were prepared using double-distilled water.

2.2. Preparation of plant extract

Fresh leaves of *K. senegalensis* (1) were properly cleaned under running tap water followed by washing with distilled water. Dried leaves (5 g) were ground into a powder and extracted with double-distilled water (ratio 1:10), the mixture was boiled for 25 min in a water bath at 70 °C. The mixture was then filtered with a Whatman Paper (No. 14) and kept in a dark bottle in a refrigerator for further analysis [27].

Figure 1: *Khaya senegalensis* leaves

2.3. Synthesis of silver nanoparticles from plant extract

In a typical experiment, 1 mM $AgNO_3$ was added to 4 mL leaf extract in a 250 mL beaker and stored in a conical flask at room temperature for the reduction of Ag^+ to Ag^0. A colour change from dark green to brown visually identifying the formation of AgNPs [28]. Green-mediated AgNPs were purified after several centrifugation at 20,000 rpm for 30 mins [29]. *K. senegalensis* synthesized AgNPs were labeled as KS-AgNPs and stored in an air-tight plastic sample vial for further use 2.

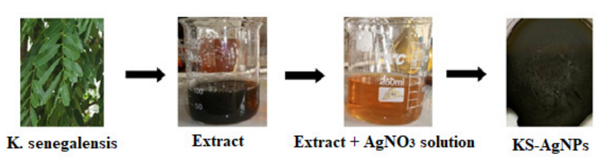

Figure 2: Reaction pathway for reduction of silver ions to silver nanoparticles using *K. senegalensis* leaves extract.

2.4. Preparation of oxidized carbon nanotubes (oCNTs)

The oCNTs was obtained by acid treatment (oxidizing) of CNTs with H_2SO_4/HNO_3 (3:1, v/v) [30]. 1 mL 0.1 M $AgNO_3$ solution was then added into 20 mL 4 mg/mL oCNTs solutions drop-wisely under assistance of ultra-sonication [31], [32]. The oxidized CNTs were successively eluted with deionized water, then by NH_4OH, water, HCl and deionized water until the pH of filtrate was stabilized.

2.5. Characterization

Green synthesized KS-AgNPs' surface plasmon resonance (SPR) peak was identified by observing UV-Visible spectra between 300 and 700 nm [33]. The phytochemical functional groups, which are found in the *Khaya senegalensis* leaves extract employed in the capping and bio-reduction of silver ions were identified using PerkinElmer Spectrum and Fourier Transform Infrared (FTIR) (PerkinElmer, Inc. Waltham, Massachusetts, USA) spectrometer in the between 400 and 4000 cm^{-1}. XRD analysis was performed using Bruker D8 X-ray diffractometer to determine the biosynthesized AgNPs crystallite size and structure. Morphological characteristics (i.e., size and shape) were examined using Scanning Electron Microscope JEOL JSM-IT 300 (JEOL) Ltd., Tokyo, Japan) working at a 30 kV voltage. Transmission electron microscopy (TEM) images were acquired on Tecnai G2 F20S-TWIN TEM (FEI Ltd., USA). The elemental composition of the green-mediated NPs, were observed using Energy Dispersive X-ray (EDX) analysis (JSM-7610F).

2.6. Photocatalytic activity

KS-AgNPs and oCNTs were used as catalysts in the degradation of industrial waste-water analyzed under sunlight for a period of three days. First, the waste-water was twice diluted with double distilled water and scanned with a UV-Vis between 300 - 700 nm wavelength [34], and the maximum wavelength obtained (590 nm) was recorded. 10 mg of KS-AgNPs and oCNTs were mixed separately with 100 mL diluted waste-water and magnetically stirred for 30 mins in order to attain equilibrium as working solution. First reading was noted after stirring. The dispersion was then exposed to sunlight irradiation and monitored between the hours of 9 am (GMT+1) and 4 pm (GMT+1). 2 mL aliquot of the suspension was taken after one hour interval, filtered and used for photocatalytic degradation evaluation. Absorbance value measurement at 580 nm was used to calculate the percentage dye degradation process according to the equation below:

$$\text{Decolourization}(\%) = \frac{A_0 - A_t}{A_0} \times 100 \quad (1)$$

where: A_0 = absorbance of the untreated and A_t = absorbance of the treated industrial waste water.

To ascertain the efficiency of both KS-AgNPs and oCNTs as a biosynthesized catalyst, selected physicochemical properties (i.e., pH, Total Dissolved Solid (TDS), Total hardness, Calcium, Magnesium, Chloride, Biological Oxygen Demand (BOD) and Total alkalinity) of the industrial waste water were assessed using standard analytical methods described by American Society for Testing and Materials (ASTM) [35].

2.7. Antibacterial activity

The antibacterial activity of the synthesized KS-AgNPs and oCNTs was investigated against Gram-positive (*Staphylococcus aureus*) and Gram-negative (*Escherichia coli*) bacteria by the Bauer-Kirby disk diffusion method [36]. Nutrient agar medium was prepared according to manufacturer's instructions by autoclaving at 121 °C for 15 mins. After sterilization, the agar was allowed to cool to about 45 °C, after which the molten agar was poured into petri dishes and allowed to solidify. The pathogens to be used as indicator organisms for antibacterial activity were inoculated on the solidified plates by using standard spread plate technique. A cork borer of about 2 mm in diameter was used to bore holes in the plates. Both the AgNPs and oCNTs to be tested for antibacterial activity were inoculated in the bored holes using a pipette. For the control, antibiotic disks were placed 2 cm away from the wall of the culture plate. The plates were incubated at 37 °C for 24 hrs, and the zone of inhibition of bacterial growth was used as a measure of susceptibility.

3. Results and Discussion

3.1. UV-Visible spectroscopy

The green-mediated reduction of the silver metal ions to KS-AgNPs was accompanied by a color change yellow to brown confirms the reduction of Ag^+ ions to Ag^o. This was monitored using UV-Vis spectrophotometer. Figure 3 shows the Surface Plasmon Resonance (SPR) with high band intensities and peaks under the visible spectrum. The KS-AgNPs showed absorbance bands within the range of 427 nm which correlate with the results reported in other literatures on the green synthesis of AgNPs [3], [37], [38], [39], [40]. The ability of the plant extracts to act as a stabilizing and capping agent can be connected to the flavonoids and protein present in *K. senegalensis* aqueous extract [41].

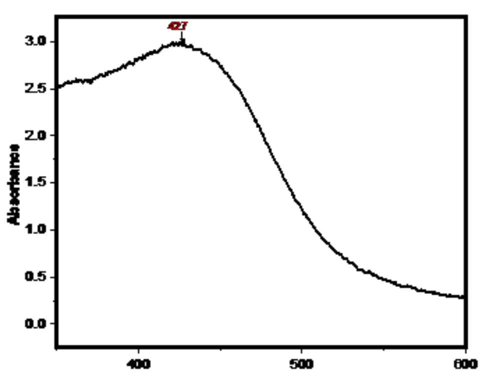

Figure 3: UV–visible spectra of green synthesized KS-AgNPs

3.2. FTIR analysis

Figure 4 shows the spectra of the aqueous extract of *K. senegalensis,* KS-AgNPs, and oCNTs. The aqueous extract of *K. senegalensis* showed characteristic peaks at 3300, and 1630 cm^{-1} which could be attributed to hydroxyl group O–H stretching [42], and C–O stretching in the carbonyl group [43] and the N–H group of amines [44], respectively. The broadband peak at 3263 cm^{-1} observed in the KS-AgNPs spectra could be attributed to the overlapping stretching mode of N–H and O–H functional groups [44]. The C–O band at 1030 cm^{-1} may be assigned to the polyols (i.e., flavones, terpenoids, and carbohydrates) present in the plant extract. The different assignments are in line with those for similar compounds that have been published in other literatures [39], [45], [46]. A broadband peak at 1549 cm^{-1} most probably corresponds to aromatic and unsaturated structure of C=C bonds was observed for oCNTs [47]. However, the acid treatment of CNTs led to the incorporation of –COOH group at 1720 cm^{-1}.

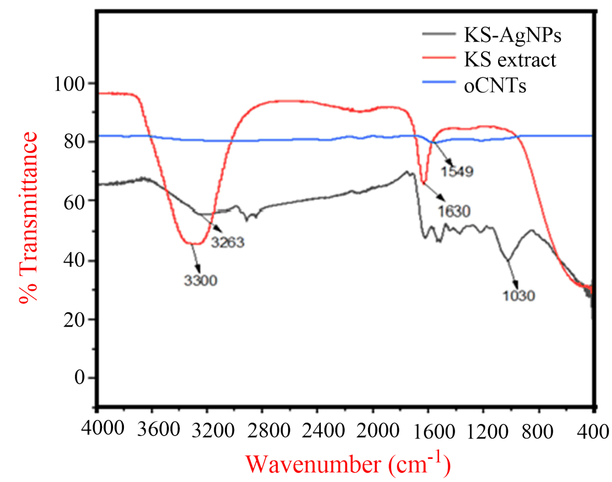

Figure 4: FTIR spectra of green synthesized KS-AgNPs, *K. senegalensis* leaf extract and oCNTs

3.3. XRD Studies

Data obtained from the silver nanoparticles were used to obtain the plot shown in Figure 5. The diffraction patterns were also used to obtained the peak positioning, however, a total of five distinct peaks at 2θ with Braggs' reflection values of 38.12°, 44.28°, 64.43°, 77.48°, and 81.54°, which corresponds to (111), (200), (220), (311), and (222) plane of faced centered cubic (fcc) lattice of silver, and compared with the standards powder diffraction card of Joint Committee on Powder Diffraction Standards (JCPDS) silver file N0. 04-0783. The most significant peak from the XRD graph is centered at 2θ = 38.117. This may be the reason why the faced-centered cubic structure of the KS-AgNPs has grown favorably [1]. In the diffraction patterns obtained in the oCNTs XRD spectra, six distinct peaks were observed with reflection values of 26.43°, 42.36°, 44.46°, 54.51°, 59.98°, and 77.40°, corresponding to (002), (100), (101), (004), (103), and (110), plane of lattice respectively. Similar result have been reported by [48]. The average particle size was estimated using the Debye-Scherrer formula as follows:

$$D = \frac{k\lambda}{\beta \cos\theta}, \qquad (2)$$

where D is the crystallite size of the AgNPs, λ is the wavelength of the X-ray source (1.54056 A), β is full width at half maximum (FWHM) of the diffraction peak in radian, k is the Scherrer constant that varies from 0.9 to 1, and θ is the Bragg angle in radian [49]. The average size was found to be 9.30 nm. One of the structural changes that causes the distortions of crystallographic materials is d-spacing (inter-planar spacing) [50]. The XRD method relies on the broadening of diffracted peaks to quantify dislocation density that happens when atoms in crystal unit cells move away from their ideal positions as a result of numerous lattice defects (strain widening) [51].

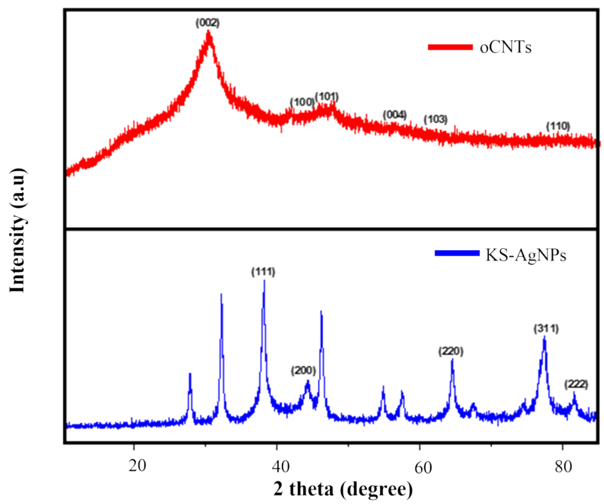

Figure 5: XRD spectra of oCNTs and KS-AgNPs

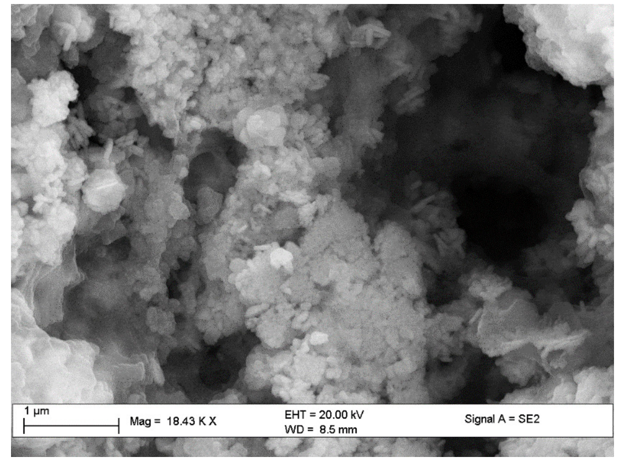

Figure 6: KS-AgNPs SEM images

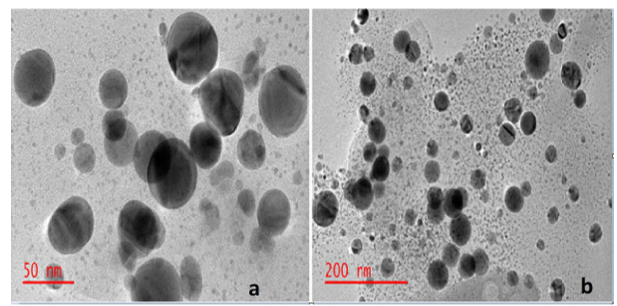

Figure 7: TEM images of green synthesized KS-AgNPs at (a) 50 nm and (b) 200 nm

3.4. SEM and TEM analysis

SEM images (Figure 6) shows the morphological character of the silver nanoparticle synthesized by the extract of *Khaya senegalensis* (African mahogany) leaves . The SEM image revealed a flake-like morphology for KS-AgNPs. Figure 7 shows the TEM images of a mono-dispersed spherical-shaped green-mediated KS-AgNPs. The interaction between the biomolecules contained in the extract suggests that the KS-AgNPs, which are uniformly distributed and mono-dispersed and have a spherical shape, have an active surface [7]. TEM analysis consequently revealed that the average size of the synthesized KS-AgNPs is 9.30 nm.

3.5. Photocatalytic activity of KS-AgNPs and oCNTs activity on industrial waste water

AgNPs and CNTs have been used as catalysts to remove halogenated organics from water, including pesticides, heavy metals, and microbes [52]. Nanoparticles are particularly effective in water treatment and disinfection to inhibit pathogenic bacteria and viruses due to their demonstrated antibacterial effectiveness [53].

In this study, photocatalytic activity of the bio-synthesized KS-AgNPs and oCNTs was assessed through decolourization of industrial wastewater under solar light after different time intervals (54 hours). The change in color was used to identify rate of pigment degradation. After 55 hours (three days) of exposure, increased decolorization was evident as color of treated industrial wastewater changed from deep orange to light orange color. A continuous decrease in the absorbance of the treated wastewater obtained using UV spectrophotometer were recorded at time interval. Steady absorbance readings obtained at the 55th hour suggested that total degradation was attained (Figure 8). The percentage degradation efficiency of the treated wastewater was highest in KS-AgNPs (86.21 %) while oCNTs had (82.14 %). Yasmin *et al.* (2020)[54] recorded close range of value for AgNPs in earlier studies. In relative comparison, KS-AgNPs, has proven to have more photocatalytic effect as shown in Figure 8, in the degradation of wastewater than oCNTs, after 55 hours of exposure. The increased absorption rate of the nano-sized silver particle distribution in KS-AgNPs compared to oCNTs may be the cause of their higher degrading efficiency [55]. More specifically, silver metal nanoparticles' highly effective catalytic activities are a result of their distinctive properties, such as their extremely small dimensions, high surface-to-volume ratio, high dispersivity, and capacity for electron transfer between the donor and acceptor electron relay systems [56], and because catalysis happens on metal surfaces during degradation, there will be a considerable increase in surface area available, which will increase the catalyst's effectiveness [57], in this case, KS-AgNPs.

The mechanism of the catalytic photo degradation of the wastewater was proposed for better understanding as shown in Figure 9.

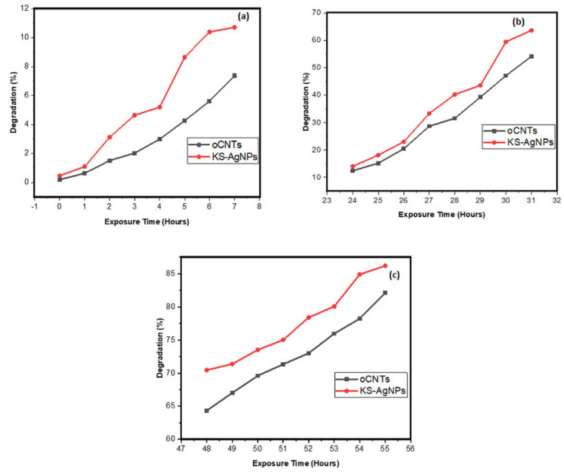

Figure 8: Effect of exposure time on the photocatalytic degradation of industrial wastewater after (a) first day (b) second day and (c) third day

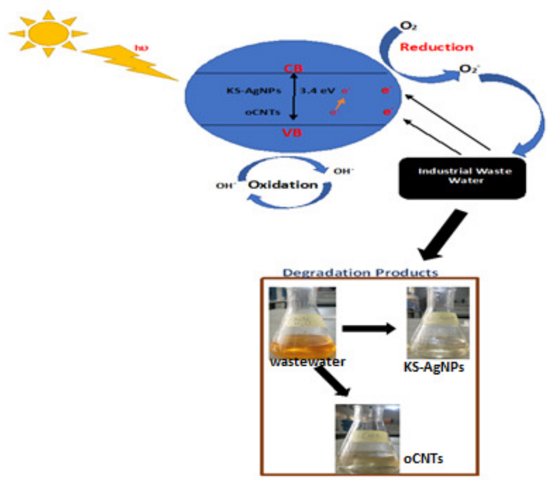

Figure 9: Mechanism of photocatalytic activity of KS-AgNPs and oCNTs

The result of photocatalytic degradation of both KS-AgNPs and oCNTs were compared with some results obtained from other literatures as shown in Table 1, with a high degradation rate observed in KS-AgNPs, confirming its excellent photocatalytic activity.

Sequel to the photocatalytic degradation of the waste water analyzed, selected physicochemical parameters were also subjected to evaluation before and after treatment with KS-AgNPs and oCNTs separately as shown in Figure 10. Comparison was also made with standard permissible limits recommended by World Health Organization (WHO). In general, the evaluation showed that both KS-AgNPs and oCNTs (in same quantity) significantly reduced the parameters analyzed. However, green-mediated KS-AgNPs greatly reduced in all parameters.

Decrease in color change of the treated industrial waste water observed can be attributed to organic pollutants adsorption. Industrial waste water pH before (10.55) and after treatment with both KS-AgNPs and oCNTs showed that KS-AgNPs had greater reduction efficiency (7.04) in comparison to oCNTs

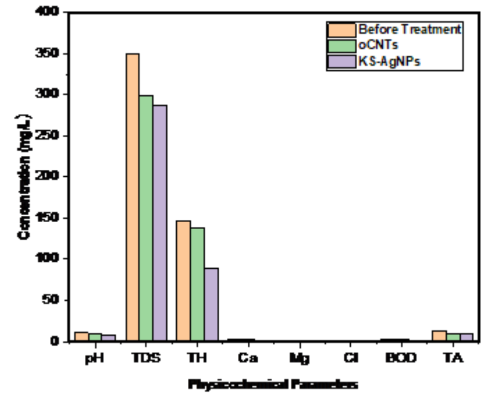

Figure 10: Plot of physicochemical assessment after treatment with KS-AgNPs and oCNTs: TDS – Total Dissolved Solids, TH – Total Hardness, Ca – Calcium, Mg – Magnesium, Cl – Chlorine, BOD – Biochemical Oxygen Demand, TA – Total Alkalinity

(9.21). The pH decrease recorded for KS-AgNPs may be due to waste water anionic species removal. Observation from KS-AgNPs was however, within WHO pH permissible limit of 6.5 – 8.5. The TDS of industrial wastewater was 350.05 mg/L, treatment with KS-AgNPs reduced the TDS concentration to 286.09 mg/L while oCNTs recorded a decrease of 299.19 mg/L. Satisfactorily, both KS-AgNPs and oCNTs reduction were lower than WHO recommended limit of 1000 mg/L for TDS in domestic water. Higher efficiency of silver nanoparticles obtained from *K. senegalensis* (KS-AgNPs) results from the reduced size of the bio-synthesized silver ion in the water.

3.6. Antibacterial Assay

Antimicrobial activity of green synthesized KS-AgNPs, oCNTs, and control antibiotics (Gentamicin and Ciprofloxacin) were tested against two selected bacteria, *Escherichia Coli* (Gram negative bacteria) *Staphylococcus aureus* (Gram positive bacteria) and investigated.

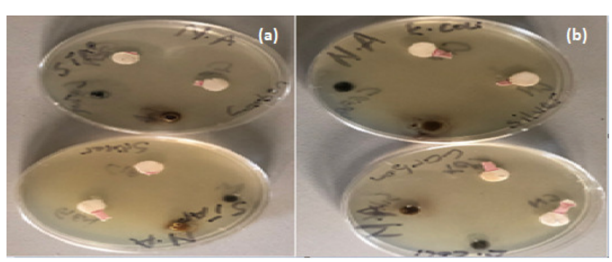

Figure 11: Inoculated plates with bore holes containing KS-AgNPs, oCNTs and known antibiotics (Gentamicin and Ciprofloxacin) before incubation for both (a) Gram (+) and (b) Gram (-) bacteria

The antibacterial activity ranged from 0 – 4 mm as observed from the results in Tables 2 and 3. oCNTs produced the lowest susceptibility to both gram-positive and gram-negative bacteria compared to KS-AgNPs, which had higher susceptibility. KS-AgNPs had susceptibility between 0.5 - 3.5 mm while oCNTs had susceptibility between 0 – 0.5 mm. The known antibiotic,

Table 1: Different catalysts and their rate of decolourization of pollutants

S/N	Catalyst	Pollutants	Effects	Reference
1.	$H_3PW_{12}O_{40}$/GO	Methyl orange, crystal violet, and Congo red	85.62 % methyl orange, 89.78 % crystal violet, and 82.62 % Congo red decolourization respectively	[58]
2.	Rambutan peel extract-ZnO nanoparticles	Methyl orange	83.99 % decolourization	[59]
3.	*Terminalia chebula* fruits extract-ZnO nanoparticles	Rhodamine B	70 % decolourization	[60]
4.	*Tinospora cordifolia*-CuO nanoparticles	Methylene blue	80 % decolourization	[61]
5.	*o-Carbon nanotubes	Industrial waste water (crude oil polluted water)	82.14 % decolourization	Present study
6.	*KS-AgNPs	Industrial waste water (crude oil polluted water)	86.21 % decolourization	Present study

Gentamicin had the highest susceptibility (4 mm), followed by the green-mediated KS-AgNPs (3.5 mm), while oCNTs had the least. The gram-negative bacteria (*E. coli*) were more susceptible to KS-AgNPs than the gram-positive bacteria (*S. aureus*), this is due to the thickness of the cell wall and cell composition. Gram (-) bacteria has thinner peptidoglycan walls compare to Gram (+) bacteria which has thicker peptidoglycan wall. However, given that small nanoparticles can easily pass through the cell membrane, susceptibility of KS-AgNPs is thought to rely on their size and shape [44]. AgNPs either adhere to the bacterial membrane or impair membrane permeability, which has an antibacterial impact, and they penetrate the cytoplasm and kill bacteria by disrupting their metabolism [62], [63]. Additionally, the destruction of bacterial pathogens may also be caused by production of free radicals by the silver nanoparticles [64].

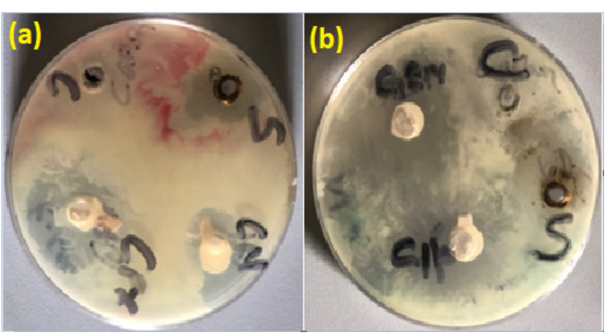

Figure 12: Antibacterial activity of (a) green-mediated KS-AgNPs and oCNTs compared with (b) antibiotics

A study by Blasco *et al.* [65] demonstrated the efficiency of AgNPs produced through green synthesis against multiple antibiotic-resistant bacterial strains, including *Staphylococcus aureus, Staphylococcus epidermidis, Streptococcus pyogenes, Klebsiella pneumoniae,* and *Salmonella typhi*, which further confirms the results obtained in this study. Moreover, AgNPs can produce pits and gaps that reduce the permeability of bacterial cell membranes, resulting in the death of the bacteria [66], [67], [68].

Table 2: Results of the antibacterial activity of the green-mediated KS-AgNPs and oCNTs

Inhibition Zone of *E. coli* bacteria against	Inhibition zone (mm)	Condition (sensitive/resistance)
Ciprofloxacin antibiotics	0	Resistance to antibiotics
KS-AgNPs	3.5	Sensitive to nanoparticle
oCNTs	0.5	Slightly sensitive

Table 3: Results of the antibacterial activity of the green-mediated KS-AgNPs and oCNTs

Inhibition Zone of *S. aureus* bacteria against	Inhibition zone (mm)	Condition (sensitive/resistance)
Gentamicin antibiotics	4	Sensitive to antibiotics
KS-AgNPs	1.5	Sensitive to nanoparticle
oCNTs	0.5	Slightly sensitive

The versatility of carbon-based nanomaterials, particularly oCNTs and graphene, has shown considerable promise in biological applications such as tissue engineering, drug delivery, and bio-imaging [69], [70]. Therefore, AgNPs are highly effective due to their clearly defined structures and substantial surface areas. By attaching AgNPs to the surface of graphene oxide or oxidized CNTs, certain potent antibacterial agents have been produced [70,71].

4. Conclusions

This study describes the quick and efficient green-mediated synthesis of KS-AgNPs employing an aqueous K. senegalensis extract as the capping and reducing agent. The color change and UV–vis adsorption confirm the reduction of Ag^+ to Ag^0. The TEM showed spherical shape with average particle size of 9.30 nm. The FTIR results confirmed the biomolecules capping and stability of the KS-AgNPs. The KS-AgNPs are stable and have excellent photocatalytic and antibacterial activities in comparison with oCNTs. The green produced KS-AgNPs method is suitable for large-scale manufacturing, quick, affordable, non-toxic, and ecologically beneficial silver nanoparticles. Overall, this work presents an effective method for creating smaller silver nanoparticles, which can be employed as antibacterial agents and to treat industrial waste water.

Acknowledgement

The authors acknowledge the Federal University of Lafia for providing the research environment for this work. Authors are also grateful to Mrs. Rasheedah Labulo for proofreading this work.

References

[1] A. U. Rahman, A. U. Khan, Q. Yuan, Y. Wei, A. Ahmad, S. Ullah, Z. U. H. Khan, S. Shams, M. Tariq & W. Ahmad, "Tuber extract of Arisaema flavum eco-benignly and effectively synthesize silver nanoparticles: Photocatalytic and antibacterial response against multidrug-resistant engineered E. coli QH4" Journal of Photochemistry & Photobiology, B: Biology **193** (2019) 31, https://doi.org/10.1016/j.jphotobiol.2019.01.018.

[2] M. A. Awad, A. A. Hendi, K. M. Ortashi, B. Alzahrani, D. Soliman, A. Alanazi, W. Alenazi, R. M. Taha, R. Ramadan, M. El-tohamy, N. Almasoud & T. S. Alomar, "Sensors and Actuators A : Physical Biogenic synthesis of silver nanoparticles using Trigonella foenum-graecum seed extract : Characterization, photocatalytic and antibacterial activities", Sensors & Actuators: A. Physical **323** (2021) 112670, https://doi.org/10.1016/j.sna.2021.112670.

[3] K. Chand, D. Cao, D. E. Fouad, A. H. Shah, A. Q. Dayo, K. Zhu, M. N. Lakhan & G. M. Shu, "Green synthesis, characterization, and photocatalytic application of silver" Arabian Journal of Chemistry **13** (2020) 8248, https://doi.org/10.1016/j.arabjc.2020.01.009.

[4] H. M. Mehwish, M. S. R. Rajoka, Y. Xiong, H. Cai, R. M. Aadil, Q. Mahmood, Z. He & Q. Zhu, "Green synthesis of a silver nanoparticle using Moringa oleifera seed and its applications for antimicrobial and sun-light mediated photocatalytic water detoxification", Journal of Environmental Chemical Engineering **9** (2021) 105290, https://doi.org/10.1016/j.jece.2021.105290.

[5] B. Thomas, B. S. M. Vithiya, T. A. A. Prasad, S. B. Mohamed, C. M. Magdalane, K. Kaviyarasu & M. Maaza, "Antioxidant and Photocatalytic Activity of Aqueous Leaf Extract Mediated Green Synthesis of Silver Nanoparticles Using Passiflora edulis", Journal of Nanoscience and Nanotechnology **19** (2019) 2640, https://doi.org/10.1166/jnn.2019.16025.

[6] Z. Noohpisheh, H. Amiri, S. Farhadi & A. Mohammadi-gholami, l P Spectrochimica Acta Part A: Molecular and Biomolecular Spectroscopy **240** (2020) 118595, https://doi.org/10.1016/j.saa.2020.118595.

[7] M. Y. Tahir, A. Ahmad, A. A. Alothman, M. S. S. Mushab & S. Ali, "Green Synthesis of Silver Nanoparticles Using Thespesia populnea Bark Extract for Efficient Removal of Methylene Blue (MB) Degradation via Photocatalysis with Antimicrobial Activity and for Anticancer Activity **202** (2022) 74.

[8] D. Thatikayala, N. Jayarambabu, V. Banothu, C. B. Ballipalli, J. Park & K. V. Rao, "Biogenic synthesis of silver nanoparticles mediated by Theobroma cacao extract : enhanced antibacterial and photocatalytic activities", Journal of Materials Science: Materials in Electronics **30** (2019) 17303, https://doi.org/10.1007/s10854-019-02077-3.

[9] G. A. Molina, R. Esparza, J. L. López-miranda, A. R. Hernández-martínez, B. L. España-sánchez, E. A. Elizalde-peña & M. Estevez, "Colloids and Surfaces B : Biointerfaces Green synthesis of Ag nano flowers using Kalanchoe daigremontiana extract for enhanced photocatalytic and antibacterial activities", Colloids and Surfaces B: Biointerfaces **180** (2019) 141, https://doi.org/10.1016/j.colsurfb.2019.04.044.

[10] V. Ravichandran, S. Vasanthi, S. Shalini, S. A. Ali Shah, M. Tripathy & N. Paliwal, "Green synthesis, characterization, antibacterial, antioxidant and photocatalytic activity of Parkia speciosa leaves extract mediated silver nanoparticles", Results in Physics **15** (2019) 102565, https://doi.org/10.1016/j.rinp.2019.102565.

[11] P. E. Fanning & M. A. Vannice, "A DRIFTS study of the formation of surface groups on carbon by oxidation", Carbon **31** (2013) 721.

[12] J. Yu, B. Yang & B. Cheng, "Noble-metal-free carbon nanotube-Cd1.0Zn0.9S composites for high visible-light photocatalytic H2-production performance", Nanoscale **4** (2012) 2670.

[13] S. Yick, A. Mai-Prochnow, I. Levchenko, J. Fang, M. Bull, A.B. Murphy & K. Ostrikow, "The effects of plasma treatment on bacterial biofilm formation on vertically-aligned carbon nanotube arrays", RSC Adv **5** (2014) 5142.

[14] T. Mocan, C.T. Matea, I. Cojocaru, I. Ilie, F.A. Tabaran, F. Zaharie, C. Iancu, D. Bartos & L. Mocan, "Photothermal treatment of human pancreatic cancer using PEGylated multi-walled carbon nanotubes induces apoptosis by triggering mitochondrial membrane depolarization mechanism", J. Cancer **5** (2014) 679.

[15] A. Al Faraj, A.P. Shaik & A. Shaik, Magnetic single-walled carbon nanotubes as efficient drug delivery nanocarriers in breast cancer murine model: noninvasive monitoring using diffusion-weighted magnetic resonance imaging as sensitive imaging biomarker", Int J Nanomed **10** (2014) 157.

[16] H. Wu, H. Shi, H. Zhang, X. Wang, Y. Yang, C. Yu, J. Du & H. Hu, "Prostate stem cell antigen antibody-conjugated multi-walled carbon nanotubes for targeted ultrasound imaging and drug delivery", Biomaterials **35** (2014) 5369.

[17] P. Wang, Y. Zhao, Y. Tian & X. Jiang, "Multiple strategies to activate gold nanoparticles as potent antibacterial agents", Nanomed Nanotechnol Biol Med. **12** (2015) 527.

[18] A. Battigelli, C. Me´nard-Moyon, T. Da Ros, M. Prato & A. Bianco, "Endowing carbon nanotubes with biological and biomedical properties by chemical modifications", Adv Drug Deliv Rev **65** (2013) 1899.

[19] R. Singh & S. Torti, "Carbon nanotubes in hyperthermia therapy", Adv Drug Deliv Rev **65** (2013) 2045.

[20] P. Wang, Y. Zhao, Y. Tian & X. Jiang, "Multiple strategies to activate gold nanoparticles as potent antibacterial agents" Nanomed Nanotechnol Biol Med **12** (2013) 527.

[21] Y. Huang, I. Lin, C. Chen, Y. Hsu, C. Chang & M. Lee, "Delivery of small interfering RNAs in human cervical cancer cells by polyethylenimine-functionalized carbon nanotubes", Nanoscale Res Lett, **8** (2013) 267.

[22] M. Martincic & G. Tobias, "Filled carbon nanotubes in biomedical imaging and drug delivery", Expert Opin Drug Deliv **12** (2015) 563.

[23] B. Zhang, H. Wang, S. Shen, X. She, W. Shi, J. Chen, Q. Zhang, Y. Hu, Z. Pang & X. Jaing, "Fibrin-targeting peptide CREKA-conjugated multi-walled carbon nanotubes for self-amplified photothermal therapy of tumor", Biomaterials **79** (2016) 46.
[24] O. Akhavan, M. Abdolahad, Y. Abdi & S. Mohajerzadeh, "Silver nanoparticles within vertically aligned multi-wall carbon nanotubes with open tips for antibacterial purposes", J. Mater. Chem. **21** (2011) 387.
[25] Y.P.I. Bai, S.J. Lee, T.S. Bae, F. Watari, M. Uo & M.H. Lee, "Aqueous dispersion of surfactant-modified multiwalled carbon nanotubes and their application as an antibacterial agent", Carbon **49** (2011) 3663.
[26] M. Karimi, N. Solati, A. Estiar, M. A. Hashemkhani, M. Kiani, P. Mohamed, E. Saeidi, A. Taheri, M. Avci, P. Aref, A. R. Amiri, M. Baniasadi & M. R. Hamblin, "Carbon nanotubes part II: A remarkable carrier for drug and gene delivery", Expert Opin Drug Deliv. **12** (2015) 1089.
[27] H. Veisi, S. Azizi & P. Mohammadi, "Green synthesis of the silver nanoparticles mediated by Thymbra spicata extract and its application as a heterogeneous and recyclable nanocatalyst for catalytic reduction of a variety of dyes in water", Journal of cleaner production **170** (2018) 1536.
[28] T. Adak, H. Swain, S. Munda, A. K. Mukherjee, M. K. Yadav, A. Sundaram & P. C. Rath, "Green silver nano-particles: synthesis using rice leaf extract, characterization, efficacy, and non-target effects", Environmental Science and Pollution Research **28** (2021) 4452.
[29] A. Baker, S. Iram, A. Syed, A. M. Elgorban, A. H. Bahkali, K. Ahmad & J. Kim, "Fruit derived potentially bioactive bioengineered silver nanoparticles", International Journal of Nanomedicine **16** (2021) 7711.
[30] M. Kumari, C. H. Liu & W. C. Wu, "Gene delivery using layer-by-layer functionalized multi-walled carbon nanotubes: design, characterization, cell line evaluation", J Mater Sci **56** (2021) 7022, https://doi.org/10.1007/s10853-020-05648-6
[31] C. Nie, C. Cheng, L. Ma, J. Deng & C. Zhao, "Mussel-Inspired Antibacterial and Biocompatible Silver-Carbon Nanotube Composites: Green and Universal Nanointerfacial Functionalization", Langmuir **32** (2016) 5955.
[32] C. Nie, Y. Yang, C. Cheng, L. Ma, J. Deng, L. Wang & C. Zhao, "Bioinspired and Biocompatible Carbon Nanotube-Ag Nanohybrid Coatings for Robust Antibacterial Applications", Acta Biomaterialia **15** (2017) 479, http://dx.doi.org/10.1016/j.actbio.2017.01.027.
[33] V. Huong & N. T. Nguyen, "Green synthesis, characterization and antibacterial activity of silver nanoparticles using Sapindus mukorossi fruit pericarp extract", Materials Today: Proceedings **42** (2021) 88.
[34] A. K. Varghese, P. P. Tamil, R. Rugmini, P. M. Shiva, K. Kamakshi & K. C. Sekhar, "Green synthesized Ag nanoparticles for bio-sensing and Photocatalytic applications", ACS omega, **5** (2020) 13123.
[35] A. Rana, S. M. S. Jilani & K. Alhooshani, "Water Quality Characterization Using ASTM Methods in an Undergraduate Advanced Instrumental Analysis Laboratory Course", Journal of Chemical Education, **98** (2021) 2919.
[36] O. Celebi, K. T. Cinisli & D. Celebi, "Antimicrobial activity of the combination (Nano-Bio) of Artemisia absinthium with copper nanoparticles", Materials Today: Proceedings **45** (2021) 3809.
[37] E. E. Elemike, D. C. Onwudiwe & A. Chinonso, "Eco-friendly synthesis of silver nanoparticles using Umbrella plant , and evaluation of their photocatalytic and antibacterial activities", Inorganic and Nano-Metal Chemistry, **50** (2020) 389, https://doi.org/10.1080/24701556.2020.1716005.
[38] A. H. Labulo, O. A. David & A. D. Terna, "Green synthesis and characterization of silver nanoparticles using Morinda lucida leaf extract and evaluation of its antioxidant and antimicrobial activity" Chemical Papers **76** (2022) 7313, https://doi.org/10.1007/s11696-022-02392-w.
[39] M. S. Aref & S. S. Salem, "Bio-callus synthesis of silver nanoparticles, characterization, and antibacterial activities via Cinnamomum camphora callus culture", Biocatalysis and Agricultural Biotechnology **27** (2020) 101689.
[40] A. Aminu & S. A. Oladepo, "Fast Orange Peel-Mediated Synthesis of Silver Nanoparticles and Use as Visual Colorimetric Sensor in the Selective Detection of Mercury (II) Ions", Arabian Journal for Science and Engineering **46** (2021) 5477.
[41] M. D. Makut, S. D. Gyar, G. R. I. Pennap & P. Anthony, "Phytochemical screening and antimicrobial activity of the ethanolic and methanolic extracts of the leaf and bark of Khaya senegalensis", African Journal of Biotechnology, **7** (2008) 1216.
[42] A. H. Labulo, E. T. Adesuji, E. E. Elemike, J. C. Onwuka & J. T. Bamgbose, "Green synthesis and growth kinetics of nanosilver under biodiversified plant extracts influence", J. Nanostruct. Chem. **5** (2015) 85.
[43] S. S. Shoor & M. Lodise, "Rapid synthesisof Au, Ag and bimetallic Au core Ag shell nanoparticles using Neem (Azadirachta indica) leaf broth", Journal of Colloid and Interface Science **275** (2006) 496.
[44] V. Kumar, S. Singh, B. Srivastava, R. Bhadouria & R. Singh, "Green synthesis of silver nanoparticles using leaf extract of Holoptelea integrifolia and preliminary investigation of its antioxidant, antiinflammatory, antidiabetic and antibacterial activities", J. Environ Chem Eng. **7** (2019) 103094, https://doi.org/10.1016/j.jece.2019.103094.
[45] S. Medina-Cruz, M. Ahmad, B. L. Swami & S. Ikram, "Green synthesis of silver nanoparticles using Azadirachta indica aqueous leaf extract", J Radiat Res Appl Sci **9** (2020) 1.
[46] S. V. Gutorova, V. V. Apyari, V. I. Kalinin, A. A. Furletov, V. V. Tolmacheva, M. V. Gorbunova & S. G. Dmitrienko, "Composable paper-based analytical devices for determination of flavonoids", Sens Actuators, B Chem **331** (2021) 129398.
[47] L. Stobinski, B. Lesiak, L. Kover, J. Toth, S. Biniak, G. Trykowski & J. Judek, "Multiwall carbon nanotubes purification and oxidation by nitric acid studied by FTIR and electron spectroscopy methods", J. Alloys and Compounds **501** (2010) 77.
[48] T. Theivasanthi & M. Alagar, "Electrolytic synthesis and characterization of silver nanopowder", arXiv:1111.0260 [physics.gen-ph] (2011), https://doi.org/10.48550/arXiv.1111.0260.
[49] S. Raja, A. Kumar, A. Hashmi & Z. Khan, "Silver nanoparticles: preparation, characterization, and kinetics", Adv Mater Lett **2** (2017) 188.
[50] V. R. Kocharyan, A. S. Gogolev, A. E. Movsisyan, A. H. Beybutyan, S. G. Khlopuzyan & L. R. Aloyan, "X-ray diffraction method for determination of interplanar spacing and temperature distribution in crystals under an external temperature gradient", J. Appl. Cryst, **48** (2015) 853, https://doi.org/10.1107/S1600576715006913.
[51] H. Farideh, J. Siestma, J. B. Amarante & M. J. Santofimia, "An improved X-ray diffraction analysis method to characterize dislocation density in lath martensitic structures", Materials Science and Engineering: A **639** (2015) 208, https://doi.org/10.1016/j.msea.2015.05.003.
[52] Z. G. Que, J. G. T. Torres, H. P. Vidal, M. A. L. Rocha, J. C. A. Pérez, I. C. López, D. D. L. C. Romero, A. E. Reyna, J. G. P. Sosa & A. A. S. Pavón, "Application of silver nanoparticles for water treatment", In Silver Nanoparticles—Fabrication, Characterization and Applications; Khan, M., Ed. IntechOpen: London, UK (2018).
[53] A. K. Bhardwaj, S. Sundaram, K. K. Yadav & A. L. Srivastav, "An overview of silver nano-particles as promising materials for water disinfection", Environ. Technol. Innov. **23** (2021) 101721.
[54] S. Yasmin, S. Nouren, H. N. Bhatti, D. N. Iqbal, S. Iftikhar, J. Majeed & H. Rizvi, "Green synthesis, characterization and photocatalytic applications of silver nanoparticles using Diospyros lotus", Green Processing and Synthesis **9** (2020) 87.
[55] Z. Khan, A. Khan, A. Shah, P. Wan, Y. Chen, G. M. Khan, A. U. Khan, K. Tahir, N. Muhammad & H. U. Khan, "Enhanced photocatalytic and electrocatalytic applications of green synthesized silver nanoparticles", Journal of Molecular Liquids **220** (2016) 248.
[56] S. K. Ghosh, S. Kundu, M. Mandal & T. Pal, "Silver and gold nanoclusters catalyzed reduction of methylene blue by Arsine in a micellar medium", Langmuir **18** (2002) 8756.
[57] C. Grogger, S. G. Fattakhov, V. V. Jouikov, M. M. Shulaeva & V. S. Reznik, "Primary steps of oxidation and electronic interactions in anodic cleavage of α,ω-diisocyanurate substituted dialkyl disulphides", Electrochimica Acta **49** (2004) 3185.
[58] L. Chen, C. Y. Zhao, X. H. Zhang, H. Li & J. Yan, "Preparation of composite material $H_3PW_{12}O_{40}$/GO and its photocatalytic degradation of methyl orange, crystal violet, and congo red", Qiqihar Univ **35** (2019) 68.
[59] T. Karnan & S. A. Selvakumar, "Biosynthesis of ZnO nanoparticles using Rambutan (Nephelium lappaceum) peel extract and their photocatalytic activity on methyl orange dye", J. Mol. Struct **1125** (2016) 358.
[60] N. Rana, S. Chand & A. K. Gathania, "Green synthesis of zinc oxide nano-sized spherical particles using Terminalia chebula fruits extract for their photocatalytic applications", Int. Nano Letter **6** (2016) 91.
[61] P. Nethravathi, M. P. Kumar, D. Suresh, K. Lingaraju, H. Rajanaika, H. Nagabhushana & S. Sharma, "Tinospora cordofolia mediated facile green synthesis of cupric oxide nanoparticles and their photocatalytic, antiox-

idant, and antibacterial properties", Mater. Sci. Semicond. Process **33** (2015) 81.

[62] E. Hoseinzadeh, P. Makhdoumi, P. Taha, H. Hossini, J. Stelling, K. M. Amjad & G. Ashraf, "A Review on Nano-Antimicrobials: Metal Nanoparticles, Methods and Mechanisms", Current Drug Metabolism **18** (2017) 120.

[63] K. Gold, B. Slay, M. Knackstedt & A. K. Gaharwar, "Antimicrobial Activity of Metal and Metal-Oxide Based Nanoparticles", Advanced Therapeutics **1** (2018) 1700033. `https://doi.org/10.1002/adtp.201700033`

[64] F. Al-Khattaf, "Gold and silver nanoparticles: Green synthesis, microbes, mechanism, factors, plant disease management and environmental risks", Saudi Journal of Biological Sciences **28** (2021) 3624, `https://doi.org/10.1016/j.sjbs.2021.03.078`.

[65] L. Blasco, A. Ambroa, R. Trastoy, I. Bleriot, M. Moscoso, L. Fernandez-Garcia, E. Perez-Nadales, F. Fernández-Cuenca, J. Torre-Cisneros & J. Oteo-Iglesias, "In vitro and in vivo efficacy of combinations of colistin and different endolysins against clinical strains of multi-drug resistant pathogens", Science Report **10** (2020) 7163.

[66] S. S. I. Abdalla, H. Katas, F. Azmi & M. F. M. Busra, "Antibacterial and Anti-Biofilm Biosynthesised Silver and Gold Nanoparticles for Medical Applications: Mechanism of Action, Toxicity and Current Status", Current Drug Delivery **17** (2020) 88.

[67] S. Majeed, M. Danish, A. H. B. Zahrudin & G. K. Dash, "Biosynthesis and characterization of silver nanoparticles from fungal species and its antibacterial and anticancer effect", Karbala Int. J. Mod. Sci. **4** (2018) 86.

[68] M. Zahoor, N. Nazir, M. Iftikhar, S. Naz, I. Zekker, J. Burlakovs, F. Uddin, A. W. Kamran, A. Kallistova & N. Pimenov, "A Review on Silver Nanoparticles: Classification, Various Methods of Synthesis, and Their Potential Roles in Biomedical Applications and Water Treatment", Water **13** (2021) 2216, `https://doi.org/10.3390/w13162216`.

[69] Q. Guo, X. Shen, Y. Li & S. Xu, "Carbon nanotubes-based drug delivery to cancer and brain", Curr. Med. Sci. **27** (2017) 635, `https://doi.org/10.1007/s11596-017-1783-z`.

[70] S. Merum, J. B. Veluru & R. Seeram, "Functionalized carbon nanotubes in bio-world: Applications, limitations and future directions", Material Science and Engineering: B **223** (2017) 43, `https://doi.org/10.1016/j.mseb.2017.06.002`.

[71] N. El-Desouky, K. Shoueir, I. El-Mehasseb & M. El-Kemary, "Synthesis of silver nanoparticles using bio valorization coffee waste extract : photocatalytic flow-rate performance, antibacterial activity , and electrochemical investigation", Biomass Conversion and Biorefinery **4** (2022) 15, `https://doi.org/10.1007/s13399-021-02256-5`.